

LOCALIZED MICROWAVE-HEATING IN SOLIDS, PLASMAS AND POWDERS, AND ITS POTENTIAL APPLICATIONS

Eli Jerby and Yehuda Meir
Faculty of Engineering, Tel Aviv University
E-mail: jerby@eng.tau.ac.il

This paper reviews the paradigm of localized microwave-heating (LMH), including effects of intentionally-induced thermal-runaway instability and hotspot formation. Experiments and theory show that LMH can be excited in metal powders, as well as in solid dielectrics. It may also generate plasmas in forms of fire-columns and fireballs, ejected directly from the molten hotspot. The dusty-plasma mechanism observed enables the production of nano-powders, directly from the substrate material (e.g. silicon or titanium). Various potential applications derived from the microwave-drill technique include for instance local heating up to >1000 K using LD MOS transistors, thermite-powder ignition (in air atmosphere and underwater), basalt melting and decomposition by dusty-plasma ejection, titania coatings, local solidification of metal powders and 3D-printing. The applicability of LMH devices, e.g. as low-cost substitute for lasers in various 3D-printing processes, is discussed.

INTRODUCTION

Microwave heating is commonly utilized in uniformly-distributed volumetric schemes, such as ovens, belt applicators, furnaces, etc. The heat-affected zone (HAZ) is typically comparable to the microwave wavelength, in the order of ~ 0.1 m or larger. Non-uniform heating patterns may accidentally evolve in such processes, hence rapidly creating local hotspots with significantly high local temperatures. Such localization effects could be harmful in microwave applications which require uniform heating, such as food processing and drying.

The microwave drill [1] intentionally utilizes the localized microwave-heating (LMH) effect by purposely exciting thermal-runaway instability [2,3] which generate a hotspot with a sub-wavelength HAZ (in the order of $\sim 10^{-3}$ m). LMH may occur in materials characterized by temperature-dependent properties which dictate faster energy absorption than diffusion rate [4]. It enables a local temperature increase to above $1,000^{\circ}\text{C}$ in a heating rate of $>100^{\circ}\text{C/s}$ in various materials. The LMH instability is ceased at the material's phase transition, to liquid, gas, or plasma. The LMH paradigm [5-7], embodied in the microwave-drill concept, is effectively extended for various other applications.

LMH effects have been demonstrated by microwave drills in various materials [8], including concrete [9,10], ceramics [11,12], and basalts [13,14]. LMH may also be useful for microwave-assisted mining [15] and concrete-recycling [16] applications. It was also found applicable for glass [17], polymers [18], and silicon [19,20]. A doping effect induced in silicon by LMH was also demonstrated [21]. In this experiment, silver and aluminum dopants were locally diffused by LMH into silicon to form a diode PN-junction.

LMH is also studied for medical applications such as tissue heating [22], bone drilling [23], interstitial treatments [24,25], ablation therapy [26], and DNA amplification [27]. Open-end coaxial applicators are used for direct heating of liquids and for activation of chemical reactions [28,29]. LMH may generate plasmoids directly from solid substrates [30-32] and produce nano-particles [33-35].

Due to the significant energy concentration, the LMH effect can be implemented by a relatively low power (in the order of ~ 0.1 kW). This feature has led to the development of solid-state LMH applicators [17]. Consequently, the LMH paradigm is also extended to compact microwave heaters, and to new applications such as incremental sintering of metal powders for 3-D printing and additive manufacturing [36], ignition of thermite reactions for material processing and combustion [37] (also in oxygen-free environments such as underwater [38,39] or in space), and to material identification by breakdown spectroscopy (MIBS) [40], as reviewed in the next sections.

THE LMH-INSTABILITY MODEL

The LMH instability can be explained in a figurative manner, as illustrated in Fig. 1 [5]. The open-end applicator is applied to a material of which the dielectric loss factor tends to increase and the thermal conductivity tends to decrease with temperature. The initial heating of the (initially) uniform material increases the temperature near the electrode tip, hence the spatial distributions of the material properties vary accordingly. The loss factor increases (and the thermal conductivity decreases) in this vicinity, hence more and more power is absorbed there, which leads to an unstable LMH response.

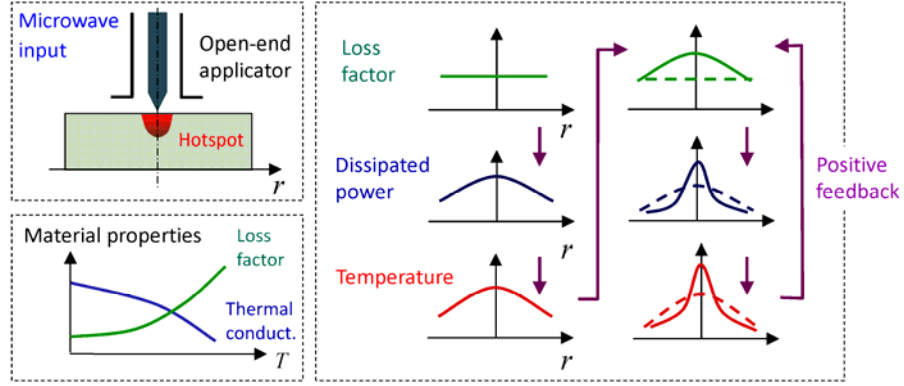


Fig. 1: The induced thermal-runaway instability and the self-focusing effect [5].

LMH models (e.g. [3], [4], [7]) are governed in general by the electromagnetic (EM) wave equation and the heat equation,

$$\nabla \times (\mu_r^{-1} \nabla \times \tilde{\mathbf{E}}) - \varepsilon_r k_0^2 \tilde{\mathbf{E}} = -jk_0 Z_0 \tilde{\mathbf{J}}, \quad (1)$$

$$\rho c_p \frac{\partial T}{\partial t} - \nabla \cdot (k_{th} \nabla T) = Q_d, \quad (2)$$

coupled together by the temperature dependent parameters and by the EM-heat dissipated power density,

$$Q_d = \frac{1}{2} \left[(\sigma + \omega \varepsilon_0 \varepsilon_r'') |\tilde{\mathbf{E}}|^2 + \omega \mu_0 \mu_r'' |\tilde{\mathbf{H}}|^2 \right], \quad (3)$$

where $\tilde{\mathbf{E}}$ and $\tilde{\mathbf{H}}$ are the electric- and magnetic-field vector components of the EM wave ($\tilde{\mathbf{H}} = j \nabla \times \tilde{\mathbf{E}} / \omega \mu_0 \mu_r$), and T is the temperature evolved in the process. The EM fields are presented as phasors in the frequency domain, where ω and k_0 are the angular frequency and free-space wave-number, respectively ($k_0 = \omega \sqrt{\varepsilon_0 \mu_0}$). The EM

wave excitation is represented by the displacement-current vector, $\tilde{\mathbf{J}}$, where $Z_0 = \sqrt{\mu_0/\epsilon_0}$ is the free-space characteristic impedance. The heated medium is characterized by its temperature-dependent parameters, μ_r , ϵ_r , σ , ρ , C_p , and k_{th} , where $\epsilon_r = \epsilon_r' - j\epsilon_r''$ and $\mu_r = \mu_r' - j\mu_r''$ are its relative complex dielectric-permittivity and magnetic-permeability, respectively, and σ is its electric conductivity. In the heat equation (2), ρ , c_p and k_{th} are the medium's actual density, heat capacity, and thermal conductivity, respectively, which may be non-uniformly changed due to the LMH effect. It is noted though that the temperature profile T is slowly varying with respect to the EM wave. The distinction between the typical time scales of the EM wave propagation (~ 1 ns) and the much slower thermal evolution (> 1 ms) allows the *two-time scale* approximation [3], hence the solution of the heat equation (2) in the time domain.

As an example for the LMH intensification effect [7], a 1-D resonator is assumed to be filled with a dielectric medium of $\epsilon_r = (4 - j0.02) \cdot [1 + (T/300 - 1)^2]$ for $T \geq T_0 = 300\text{K}$, $\rho c_p = 1 \text{ J/cm}^3 \text{ K}$, and $L = 6 \text{ cm}$. The resonator is excited by a 2.45-GHz microwave generator ($\sim 1 \text{ kW}$), and the non-resonating fundamental axial mode $n = 1$ is imposed by the equivalent current $\tilde{J}_x(z)$. The coupled solution of Eqs. (1) and (2) shows that higher-order modes are dynamically evolved during the non-uniform microwave heating [7]. The temperature-dependent dielectric permittivity (modified along the resonator) is coupled to the higher-order modes. These enable the sharper sub-wavelength intensification of the EM dissipated power $Q_d(z, t)$, initially distributed as the original fundamental mode (with a $\sin^2(\pi z/L)$ profile). As the LMH instability proceeds, Q_d becomes significantly intensified and confined at the hotspot region, as shown in Fig. 2a. The localized temperature profile is sharpened accordingly to intensify the hotspot, as shown in Fig. 2b.

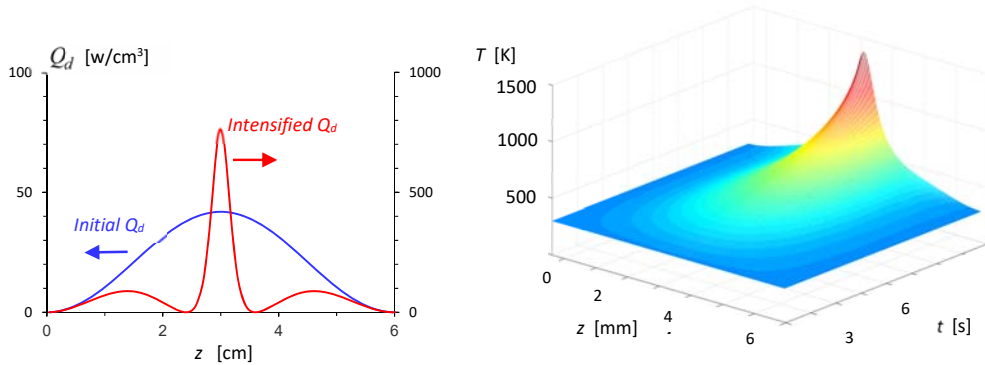


Fig. 2: A numerical example of LMH in a 1-D cavity [7]. (a) Initial and final profiles of the dissipated power density Q_d along the cavity, from the fundamental-mode excitation to the LMH instability and hotspot. (b) The localized temperature profile along the cavity, and the hotspot evolved.

In another example [6], an arbitrary material is placed in front of a waveguide aperture. The LMH effect is seen in Fig. 3 by the temperature profile and also by the focusing-like convergence of the Poynting vector towards the hotspot. The LMH effect enables a wide range of applications in a variety of fields. Several examples are further discussed in the next sections.

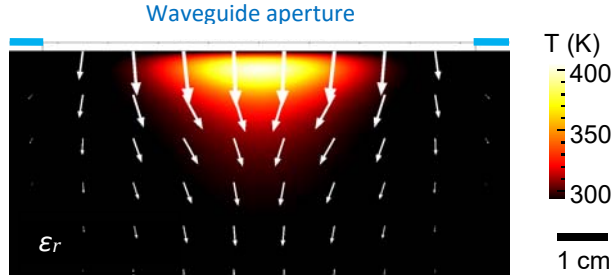


Fig. 3: A numerical simulation of a hotspot evolved in an arbitrary material placed in front of a waveguide aperture ($\epsilon_r = 2.0 - j0.1(T - 290)$ and WR340, respectively) [6]. The LMH effect is evident by the temperature profile, as well as the focusing-like convergence of the Poynting vector (denoted by the white arrows).

THE MICROWAVE DRILL

A silent microwave-drill for concrete was recently developed [10] with the capability to drill 12-mm diameter, >25-cm deep holes. Delicate microwave drilling operations were also demonstrated (in a ~1-mm diameter range), for instance by relatively low-power (~0.1 kW) LMH applied to soda-lime glass plates (of 1-4 mm thickness) [17]. The simulation of the LMH evolution in these cases by Eqs. (1-3), using Comsol Multiphysics™, agrees well with the experimental measurements [17]. A simulated hotspot profile is shown for instance in Fig. 4a, with an image of a hole made in glass by a miniature microwave-drill operated in similar conditions (Fig. 4b).

The relatively low power needed for open-end coaxial applicators to reach LMH intensification in millimeter scales (typically below ~0.2 kW) makes solid-state generators (e.g. LDMOS [17]) suitable as sources for LMH applicators. These compact schemes enable a new range of portable LMH intensifiers.

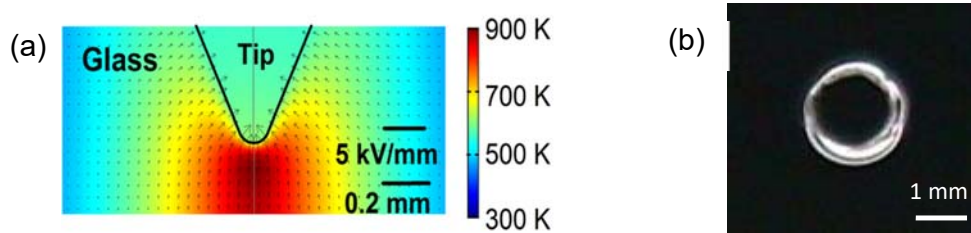


Fig. 4: LMH effect in glass irradiated by a coaxial open-end applicator using an LDMOS-based microwave-drill [17]: (a) The simulated spatial temperature and electric-field distributions at the hotspot, and (b) an image of a ~1.6-mm \varnothing hole made by LMH in glass.

PLASMA EJECTION FROM SOLIDS

A typical experimental setup used for LMH-plasma experiments is schematically shown in Figs. 5a,b. It consists of a microwave cavity (made e.g. of a WR340 waveguide) with openings in microwave cutoff for diagnostic purposes. A movable electrode directs the microwave energy locally into the substrate. The microwave power is generated by a 2.45-GHz, 1-kW magnetron unit, fed by a controllable switched-mode power-supply (or alternatively by an LDMOS-FET oscillator [17]).

Dusty plasmas in forms of fireballs and fire-columns as shown in Fig. 6a can be ejected by LMH directly from hotspots evolved in solid substrates made of various dielectric and metallic materials [31-35]. The intensified LMH-plasma process begins

with a hotspot formation as for microwave drilling. For plasma ejection, however, the electrode is lifted up (rather than pushed in) in order to detach the molten drop from the surface, and to further inflate it to a form of a buoyant fireball.

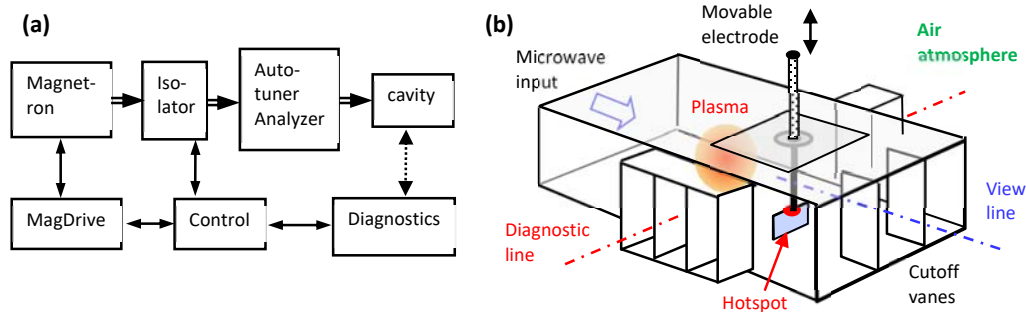


Fig. 5: A typical experimental setup for LMH-plasma generation [32]: (a) A block diagram of the experimental instrumentation, and (b) the microwave cavity.

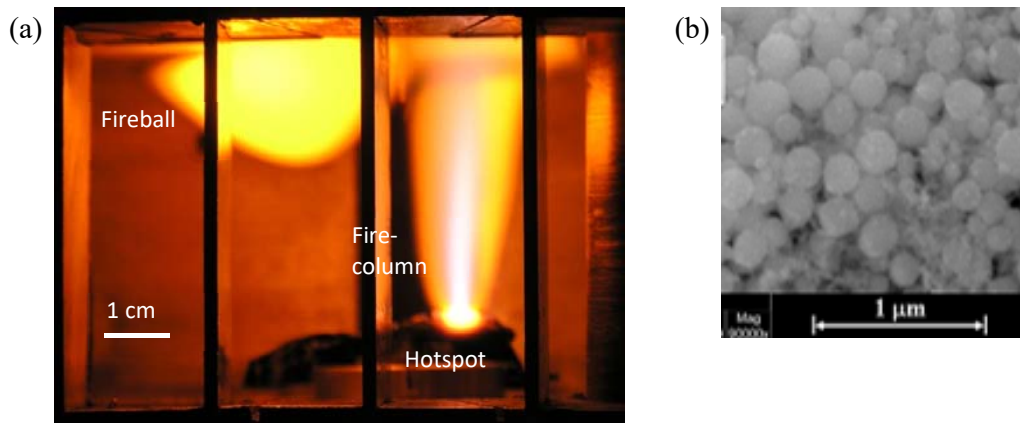


Fig. 6: Plasmoids ejected by LMH from a hotspot in glass [31]. (a) The hotspot in the solid substrate, the fire-column ejected, and the secondary fireball evolved (captured together). (b) Nano-particles produced by LMH generated dusty plasma, as observed by SEM.

Beside their resemblance to natural ball-lightning phenomena, fireballs and fire-columns as shown in Fig. 6a, may also have practical importance, e.g. as means to produce nano-particles (Fig. 6b) directly from various substrate materials, such as silicon, glass, ceramics, copper, titanium, etc. [31-35]. Nanoparticles were observed in these and other materials, both by *in-situ* synchrotron small-angle X-ray scattering (SAXS) of the dusty plasma, and by *ex-situ* SEM observations of the nano-powders collected after the processes. Particle of various sizes, shapes, and number densities have been obtained (typically of $<0.1 \mu\text{m}$ size and $\sim 10^{16} \text{m}^{-3}$ number density within the dusty plasma). The LMH generated plasma can also be used for material identification [40] by atomic emission spectroscopy of the light emitted by the plasma ejected from the hotspot (similarly to the laser induced breakdown spectroscopy (LIBS)).

DOPING AND SURFACE TREATMENT BY LMH

The feasibility of local doping of silicon by silver and aluminum using LMH has been demonstrated [21] in experiments in which the dopant material was incorporated in the electrode tip, and diffused into the locally heated bulk, in order to form a sub-micron

junction. The doping depth was determined by the applied microwave power. Oxidation effects were also observed in these experiments, conducted in air atmosphere. Chemical reactions applied by LMH for surface treatment may include also thermite reactions for rust conversion to iron [37]. These LMH techniques open new possibilities for a variety of surface treatments and local surface processing.

LMH OF METAL POWDERS

Coupling mechanisms of microwaves and metal powders are known in the literature in various volumetric schemes [41]. Recent experiments show that metal powders with negligible dielectric losses can also be effectively heated and incrementally solidified by localized microwaves [36]. This LMH effect is attributed to the time-varying magnetic component of the EM field, and to the eddy currents induced in the metal-powder particles, as illustrated in Fig. 7a [41]. This effect is intensified by the micro-powder geometry, and it also occurs in diamagnetic metals such as copper. The heat is generated due to the metal electric resistivity, which impedes the eddy currents.

In magnetic-like heating of metallic powders, the LMH effect is not characterized by thermal-runaway instability since the temperature tends to stabilize at ~ 700 K due to the particle necking and consolidation effects.

LMH IGNITION OF THERMITE REACTIONS

Powder mixtures, such as pure aluminum and magnetite powders, may generate energetic thermite reactions. These could be useful for a variety of combustion and material processing applications. However, their usage is yet limited by the difficult ignition of these reactions. It was recently found that ignition of thermite reactions is feasible by intensified LMH [37]. The power required for thermite ignition by LMH is ~ 0.1 -kW for a ~ 3 -s period, which could be provided by a solid-state microwave generator.

The thermite mixture exhibits both dielectric and magnetic loss mechanisms. The magnetic LMH is implemented by a short-end applicator, which enhances the magnetic field in front of it. It yields a faster heating rate than the open-end, dielectric-LMH applicator, up to the Curie temperature at 858K, where the magnetic losses significantly decrease. Integrating both magnetic and electric LMH mechanisms by a hybrid applicator enables the thermal-runaway instability and the thermite ignition [37]. These experiments also demonstrate the feasibility of cutting and welding by relatively low-power LMH. The initiation of the intense exothermic reaction in thermites, as shown in Fig. 7b, also demonstrates an example for LMH ignition of other high-temperature self-propagating syntheses (SHS).

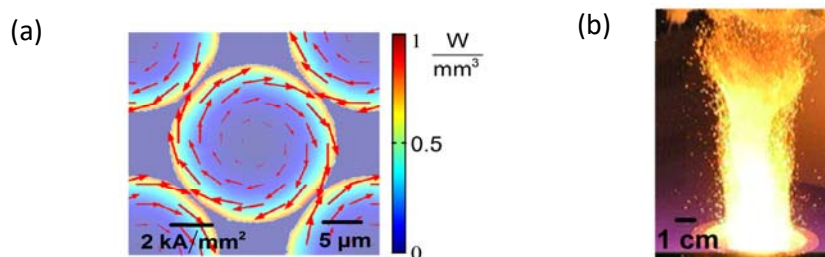


Fig. 7: LMH of metallic powders. (a) Eddy currents induced in copper powder [41]. (b) A thermite flame ignited by LMH intensification [37].

Due to their zero-oxygen balance, exothermic thermite reactions may also occur underwater. However, this feature is also difficult to utilize because of the hydrophobic properties of the thermite powder, and its tendency to agglomerate on the water surface, rather than to sink into the water. The recently discovered bubble-marble (BM) effect [38] enables the insertion and confinement of a thermite-powder batch into water by a static magnetic field, and its ignition by LMH underwater [39]. Potential applications of this underwater combustion effect may include wet welding, thermal drilling, detonation, thrust generation, material processing, and composite-material production. These could be implemented in other oxygen-free environments as well, such as the outer space.

LMH POTENTIAL FOR 3D PRINTING

The LMH effect in metal powders is also associated with internal micro-plasma breakdowns between the particles, which leads to local melting and solidification of the metal powder. This effect enables a potential technique for stepwise 3D printing and additive manufacturing (AM) [36]. The solidified drop of metal powder is placed in this technique as a building block on top of the previously constructed block in a stepwise AM process, as illustrated in Fig. 8a. A rod constructed by LMH-AM from bronze-based powder is shown in Fig. 8b [36]. A similar process using magnetic fixation of iron powder has also been demonstrated [42].

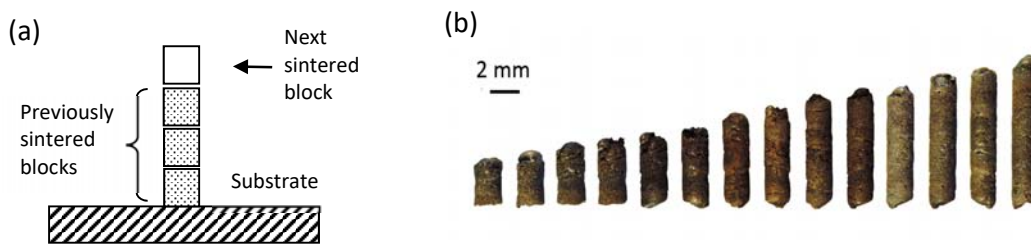


Fig. 8: Additive manufacturing (3D printing) of metal powders by LMH [36]: (a) A conceptual scheme of the stepwise LMH-AM process. (b) A 2-mm \varnothing rod constructed in 14 consequent steps from bronze-based powder.

DISCUSSION

The LMH paradigm presented in this paper extends the common microwave-heating technology to HAZ sizes much smaller than the microwave wavelength. In LMH, the microwave radiation is self-focused intentionally into a millimeter-size hotspot hence melting or evaporating it locally. Further to melting and evaporation, dusty plasma rich of nanoparticles can be ejected directly from the solid substrate.

The LMH does not require a cavity or a closed chamber, and it can be implemented by conventional low-cost microwave generators. In the low-power range, LMH can be implemented even by a solid-state generator. The LMH paradigm incorporates the theory of the induced thermal-runaway instability together with the experimental studies of local melting and plasma ejection effects. The LMH is applicable to dielectrics and metals as well, in solid, powder, and liquid forms. Figure 9 shows a conceptual scheme of the LMH relevance to the various matter states and to their transitions, and indicates some of the applications related to them.

The LMH technique can be considered as a partial substitute for some laser-based applications (e.g. drilling, cutting, joining, surface treatment, material identification,

rapid manufacturing) to a limited extent. While LMH may provide low-cost and compact solutions in this regard, it requires a physical contact with the object and its ~1mm resolution is inferior with respect to lasers. It is expected therefore that LMH will find applications in ranges of larger volumes and rougher missions, as a complementary means to the relatively more accurate and expensive lasers.

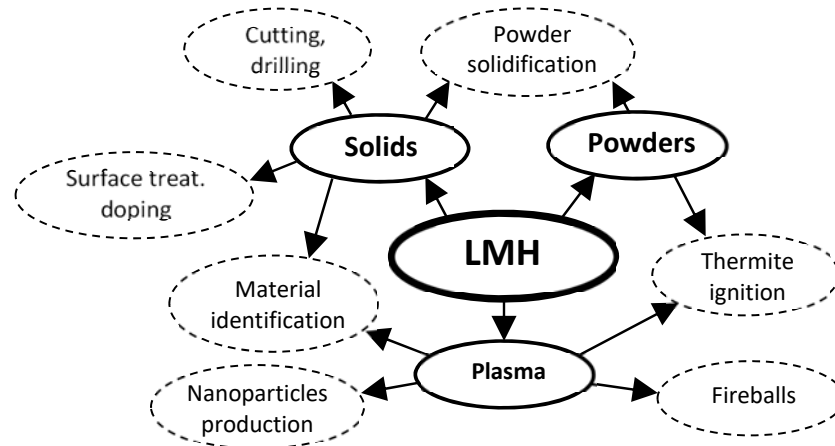


Fig. 9: LMH relevance to various matter states and transitions, and to their related applications [5].

ACKNOWLEDGEMENTS

This research was supported in part by The Israel Science Foundation (Grant Nos. 1270/04, 1639/11, and 1896/16).

REFERENCES

1. E. Jerby, V. Dikhtyar, O. Aktushev and U. Groszlick, "The microwave drill," *Science*, Vol. 298, pp. 587-589, 2002.
2. G. Roussy, A. Bennani, J. Thiebaut, "Temperature runaway of microwave irradiated materials," *Jour. Appl. Phys.*, Vol. 62, pp. 1167-1170, 1987.
3. E. Jerby, O. Aktushev, V. Dikhtyar, "Theoretical analysis of the microwave-drill near-field localized heating effect," *Jour. Appl. Phys.*, Vol. 97, Art. No. 034909, pp. 1-7, 2005.
4. Y. Alpert, E. Jerby, "Coupled thermal-electromagnetic model for microwave heating of temperature-dependent dielectric media," *IEEE Trans. Plasma Sci.*, Vol. 27, pp. 555-562, 1999.
5. Y. Meir, E. Jerby, "The localized microwave-heating (LMH) paradigm – Theory, experiments, and applications," *Proc. 2nd Global Congress on Microwave-Energy Applications*, 2GCMEA, pp. 131-145, Long Beach, California, July 23-27, 2012.
6. Y. Meir, E. Jerby, "The localized microwave-heating (LMH) paradigm – Theory, observations, and applications," *Proc. 15th Int'l Conf. Microwave & High-Frequency Heating*, AMPERE 2015, Krakow, Poland, Sept. 14-17, 2015.
7. E. Jerby, "Localized microwave-heating intensification – A 1-D model and potential applications," *Chemical Engineering and Processes (CEP)*, Vol. 122, pp. 331-338, 2017.
8. E. Jerby, O. Aktushev, V. Dikhtyar, P. Livshits, A. Anaton, T. Yacoby, A. Flax, A. Inberg, D. Armoni, "Microwave drill applications for concrete, glass and silicon" *Proc. 4th World Congress Microwave & Radio-Frequency Applications*, pp. 156-165, Nov. 4-7, 2004, Austin, Texas.
9. E. Jerby, V. Dikhtyar, "Drilling into hard non-conductive materials by localized microwave radiation," 8th Int'l Conf. Microwave & High-Frequency Heating, Bayreuth, Sept. 4-7, 2001, in *Advances in Microwave and Radio-Frequency Processing*, M. Willert-Porada, Ed., Springer, 2006, pp. 687-694.
10. E. Jerby, Y. Meir, Y. Nerovny, O. Korin, R. Peleg, Y. Shamir, "Silent microwave-drill for concrete," *IEEE Trans. Microwave Theory and Techniques*, Vol. 66, pp. 522-529, 2018.

11. E. Jerby, V. Dikhtyar, O. Aktushev, "Microwave drill for ceramics," *Amer. Ceramic Soc. Bull.*, Vol. 82, pp. 35-37, 2003.
12. E. Jerby, A.M. Thompson, "Microwave drilling of ceramic thermal barrier coatings," *Jour. Amer. Ceram. Soc.*, Vol. 87, pp. 308-310, 2004.
13. E. Jerby, Y. Meir, M. Faran, "Basalt melting by localized-microwave thermal-runaway instability," *Proc. AMPERE 14th Int'l Conf. Microwave & High Frequency Heating*, pp. 255-258, Nottingham, UK, Sept. 16-19, 2013.
14. E. Jerby, Y. Shoshany, "Fire-column-like dusty-plasma ejected from basalt by localized microwaves," *45 IEEE Int'l Conf. on Plasma Sciences, ICOPS-2018*, Denver, Colorado, June 24-28, 2018.
15. G. Wang, P. Radziszewski, J. Ouellet, "Particle modeling simulation of thermal effects on ore breakage," *Comput. Mater. Sci.*, Vol. 43, pp. 892-901, 2008.
16. N. R. Lippiatt, F. S. Bourgeois, "Recycling-oriented investigation of local porosity changes in microwave heated-concrete," *KONA Powder & Particle Jour.*, Vol. 31, pp 247-264, 2014.
17. Y. Meir and E. Jerby, "Localized rapid heating by low-power solid-state microwave-drill," *IEEE Trans. Microwave Theory & Tech.*, vol. 60, pp. 2665-2672, 2012.
18. J. B. A. Mitchell, E. Jerby, Y. Shamir, Y. Meir, J. L. LeGarrec, M. Sztucki, "Rapid internal bubble formation in a microwave heated polymer observed in real-time by X-ray scattering," *Polym. Degradation Stab.*, Vol. 96, pp. 1788-1792, 2011.
19. X. Wang, W. Liu, H. Zhang, S. Liu, Z. Gan, "Application of microwave drilling to electronic ceramics machining," *7th Int'l Conf. Electronics Packaging Technology*, Proc. Article # 4198945, pp. 1-4, Aug. 26-29, 2006, Shanghai, China.
20. R. Herskowits, P. Livshits, S. Stepanov, O. Aktushev, S. Ruschin, E. Jerby, "Silicon heating by a microwave-drill applicator with optical interferometric thermometry," *Semicond. Sci. Tech.*, Vol. 22, pp. 863-869, 2007.
21. P. Livshits, V. Dikhtyar, A. Inberg, A. Shahadi, E. Jerby, "Silicon doping by a point-contact microwave applicator," *Microelectron. Eng.*, Vol. 88, pp. 2831-2836, 2011.
22. A. Copty, F. Sakran, M. Golosovsky, D. Davidov, A. Frenkel, "Low power near-field microwave applicator for localized heating of soft matter," *Appl. Phys. Lett.*, Vol. 84, pp. 5109-5111, 2004.
23. Y. Eshet, R. Mann, A. Anaton, T. Yacoby, A. Gefen, E. Jerby, "Microwave drilling of bones," *IEEE Trans. Biomedical Eng.*, Vol. 53, pp. 1174-1182, 2006.
24. T. Z. Wong, B. S. Trembly, "A theoretical model for input impedance of interstitial microwave antennas with choke," *Int. Jour. Radiat. Oncol. Biol. Phys.*, Vol. 28, pp. 673-682, 1994.
25. I. Longo, G. B. Gentili, M. Cerretelli, N. Tosoratti, "A coaxial antenna with miniaturized choke for minimally invasive interstitial heating," *IEEE Trans. Biomed. Eng.*, Vol. 50, pp. 82-88, 2003.
26. P. Keangin, P. Rattanadecho, "Analysis of heat transport on local thermal non-equilibrium in porous liver during microwave ablation," *Int'l Jour. Heat Mass Trans.*, Vol. 67, pp. 46-60, 2013.
27. A. Kempitiya, D. A. Borca-Tasciuc, H. S. Mohamed, M. M. Hella, "Localized microwave heating in micro-wells for parallel DNA amplification applications," *Appl. Phys. Lett.*, Vol. 94, Art. No. 064106, pp. 1-3, 2009.
28. F. Marken, "Chemical and electro-chemical applications of in situ microwave heating," *Annu. Rep. Prog. Chem.*, Sect. C, Vol. 104, pp. 124-141, 2008.
29. Y. Tsukahara, A. Higashi, T. Yamauchi, T. Nakamura, M. Yasuda, A. Baba, Y. Wada, "In situ observation of nonequilibrium local heating as an origin of special effect of microwave on chemistry," *Jour. Phys. Chem. C*, Vol. 114, pp. 8965-8970, 2010.
30. V. Dikhtyar, E. Jerby, "Fireball ejection from a molten hot-spot to air by localized microwaves," *Phys. Rev. Lett.*, Vol. 96, Art. No. 045002, pp. 1-4, 2006.
31. Y. Meir, E. Jerby, Z. Barkay, D. Ashkenazi, J. B. A. Mitchell, T. Narayanan, N. Eliaz, J-L LeGarrec, M. Sztucki, O. Meshcheryakov, "Observations of ball-lightning-like plasmoids ejected from silicon by localized microwaves," *Materials*, Vol. 6, pp. 4011-4030, 2013.
32. E. Jerby, "Microwave-generated fireballs," *Encyclopedia of Plasma Technology*, Taylor and Francis, 2017, pp. 819-832.
33. J. B. Mitchell, J. L. LeGarrec, M. Sztucki, T. Narayanan, V. Dikhtyar, E. Jerby, "Evidence for nanoparticles in microwave-generated fireballs observed by synchrotron X-ray scattering," *Phys. Rev. Lett.*, Vol. 100, Art. No. 065001, pp. 1-4, 2008.
34. E. Jerby, A. Golts, Y. Shamir, S. Wonde, J. B. A. Mitchell, J. L. LeGarrec, T. Narayanan, M. Sztucki, D. Ashkenazi, Z. Barkay, "Nanoparticle plasma ejected directly from solid copper by localized microwaves," *Appl. Phys. Lett.*, Vol. 95, Art. No. 191501, 2009.

35. S. Popescu, E. Jerby, Y. Meir, Z. Barkay, D. Ashkenazi, J. B. A. Mitchell, J-L. Le Garrec, T. Narayanan, "Plasma column and nano-powder generation from solid titanium by localized microwaves in air," *Jour. Appl. Phys.*, Vol. 118, Art. No. 023302, 2015.
36. E. Jerby, Y. Meir, A. Salzberg, E. Aharoni, A. Levy, J. Planta Torralba and B. Cavallini, "Incremental metal-powder solidification by localized microwave-heating and its potential for additive manufacturing," *Additive Manufacturing*, Vol. 6, pp. 53-66, 2015.
37. Y. Meir, E. Jerby, "Thermite-powder ignition by electrically-coupled localized microwaves," *Combust. Flame*, Vol. 159, pp. 2474-2479, 2012.
38. Y. Meir, E. Jerby, "Insertion and confinement of hydrophobic metallic powder in water: The bubble-marble effect," *Phys. Rev. E*, Vol. 90, Art. No. 030301(R), pp. 1-4, 2014.
39. Y. Meir, E. Jerby, "Underwater microwave ignition of hydrophobic thermite powder enabled by the bubble-marble effect," *Appl. Phys. Lett.*, Vol. 107, Art. No. 054101, pp. 1-4, 2015.
40. Y. Meir, E. Jerby, "Breakdown spectroscopy induced by localized microwaves for material identification," *Microw. Opt. Tech. Lett.*, Vol. 53, pp. 2281-2283, 2011.
41. T. Galek, K. Porath, E. Burkel, U. Van Rienen, "Extraction of effective permittivity and permeability of metallic powders in the microwave range," *Modell. Simul. Mater. Sci. Eng.*, Vol. 18, Art. No. 025015, pp. 1-13, 2010.
42. M. Fugenfirov, Y. Meir, A. Shelef, Y. Nerovni, E. Aharoni, E. Jerby, "Incremental solidification (towards 3D-Printing) of magnetically-confined metal-powder by localized microwave heating," *Int'l Journal Computation & Mathematics in Electrical and Electronic Eng. (COMPEL)*, in Press.